Proceedings of the IAEA Advisory Group Meeting on Nuclear and Atomic Data for Radiotherapy and Radiobiology, Rijswijk, the Netherlands, Sept. 16-20, 1985 (in press).

SECONDARY CHARGED PARTICLE SPECTRA AND KERMA CALCULATIONS

J. J. Coyne and H. M. Gerstenberg

National Bureau of Standards
Gaithersburg, MD 20899

and

Dr. L. A. Hennen

Radiobiological Institute TNO
P.O. Box 5815, 2280 HV Rijswijk, The Netherlands
and
Interuniversity Institute of Radiopathology
and Radiation Protection
Leiden, The Netherlands

DISCLAIMER

1. INTRODUCTION

The calculation of kerma factors from known cross sections is not as simple as is often implied. The kerma factors are strongly influenced by the reaction mechanism assumed. An important example of this dependence on the reaction mechanism is the contribution of the $^{12}C(n,n')3\alpha$ reaction to the total kerma in carbon. First, a short review will be given of the ENDF/B-V[1] carbon cross sections which were used in the calculation of carbon kerma factors reported in the ICRU Report 26[2,3]. Using the reaction channels implied in the ENDF/B-V evaluation, the contribution of various reactions to the total kerma factors in carbon will be given.

A detailed analysis of the reaction mechanisms which could contribute to the $(n,n')3\alpha$ reaction in carbon has been carried out. First their contribution to kerma, independent of cross section, will be calculated and then the initial spectra of alpha particles produced by the various reaction mechanisms will be given. A discussion of possible ways of experimentally distinguishing the reaction mechanisms will be made by comparing their different initial spectra and their variation in kerma with neutron energy. Finally, the event-size spectra for tissue-equivalent proportional counters will be presented, giving only the contributions from the $(n,n')3\alpha$ reaction and its various possible reaction channels.

2. CARBON CROSS SECTIONS AND VARIOUS CONTRIBUTIONS TO KERMA FACTORS IN THE ENERGY REGION BETWEEN 11 AND 20 MEV

The cross sections for the various carbon reactions are given (in terms of the percent of the total carbon cross section) in Table 1; these data were obtained from the ENDF/B-V evaluation. The total non-elastic cross section (the difference between the total and elastic cross section) is approximately 40% of the total cross section in this energy region. The total cross section, σ_T, is thought to be known to 2% and the elastic cross section, σ_e, to 3-5%. All of the other cross sections must then add up to the difference $(\sigma_T - \sigma_e)$ within some error. For example, if it is assumed that all of the other cross sections are known to some accuracy then it is implied that the $(n,n')3\alpha$ is known to a given accuracy and this assumption will have its implications on the accuracy of the contributions to the kerma factors. A detailed study of the implications of these correlations will soon be undertaken when we re-evaluate the kerma factors for carbon in the near future.

Table 2 gives the percent of the total kerma factor due to various interactions in carbon resulting from the ENDF/B-V cross sections. The $(n,n')3\alpha$ cross section contributes substantially to the total kerma factor in the energy range between 11 and 20 MeV region. However, the (n,α) reaction also is an important contributor and gives a larger contribution per unit cross section then any other reaction in this energy region. ENDF/B-V assumes most of the cross section for $(n,n')3\alpha$ involves the excited states of ^{12}C(7.653 MeV, 9.638 MeV, 10.3 MeV, etc.). The one channel which ENDF/B-V labeled as channel 91, has been taken as going through an excited state of ^{9}Be(2.43 MeV).

3. REACTION MECHANISMS CONTRIBUTING TO THE REACTION $^{12}C(n,n')3\alpha$

If the four-body breakup of the intermediate ^{13}C compound state is excluded then there are eight different reaction mechanisms which can contribute to the $(n,n')3\alpha$ reaction and they are given in Table III. The assumption of one of these mechanisms with the implied excited states gives a definite dependence of kerma factor on neutron energy per unit cross section and also gives a definite initial alpha-particle spectrum. First, the dependence of kerma per unit cross section as a function of neutron energy is given. Figure 1 gives the variation of the kerma factor per unit cross section for various excited states of ^{12}C. Since the kerma factors for the reaction channels labeled 1 and 7 in Table 3 are the same, this figure applies to both of these channels. Only four excited states are shown but there are a total of 17 excited states given in ENDF/B-V. As expected, the kerma factor, as well as the threshold energy, is higher for higher excited states. For comparison the contribution of the reaction $^{12}C(n,\alpha)^{9}Be$(G.S.) is also shown in Figure 1. This reaction is the strongest contributor to the kerma factor per unit cross section in carbon. Also given are the results for elastic scattering, which is a relatively weak contributor to kerma factor per unit cross section.

Figure 2 gives similar data for the channels labeled 2 and 8. These two channels are similar in that they involve intermediate species of ^{9}Be in excited states, but differ in that channel 2 involves two two-body decays while channel 8 involves a three-body decay. When ^{9}Be is in the 2.43 MeV excited state there is little difference in the results for NQ = 2 and 8, but when ^{9}Be is in the 6.66 MeV excited state there is a larger difference and the results for NQ = 2 are the lowest. The results for $^{12}C(n,\alpha)^{9}Be$ are again given and it is seen that the kerma for the (n,α) reaction is the highest of all and the NQ = 2, E^{*} = 6.66 MeV is the lowest. For channels 2 and 8, the kerma factor per unit cross section increases much more rapidly as a function of neutron energy than for channels 1 and 7, where the inelastic neutron is the first particle out and the excited states of ^{12}C are involved.

Figure 3 gives the results for the other four reaction channels. The channels labeled 3, 4, and 6 involve ^{5}He as an intermediate state and the kerma factor per unit cross section varies approximately like that of channel 2 (see Fig. 2) with the 2.43 MeV excited state of ^{9}Be. The results for NQ = 5 are of interest because this reaction channel has the lowest threshold of all the reactions and is the closest to four-body breakup, since there is only a small positive Q of .0947 MeV in the decay of ^{8}Be. Near threshold, this is the only reaction which can take place and the increase in kerma factor per unit cross section as a function of neutron energy is less than that for the other reaction channels except for channels 1 and 7.

4. THE ALPHA PARTICLE ENERGY SPECTRA

The alpha-particle energy spectrum produced by 14.1 MeV neutrons will now be discussed. Data on these spectra at other neutron energies are available and will be published in a more complete paper. Figure 4 compares the alpha-particle spectra at 14.1 MeV neutron energy for channels 1 and 7, when an excited state of 9.638 MeV in ^{12}C is assumed. These two spectra produce the same kerma and are only slightly different in shape. Channel 1 and 7 differ only in that channel 7 involves a three-body decay, while channel 1 has a series of two two-body decays. Some difference in shape will be observed only when the neutron energy is just above the threshold for exciting the particular state of ^{12}C. Figure 5 gives such a case for E^{*} equal 12.25 MeV and E_{n} equal 14.1 MeV. For NQ = 1, the high-energy alpha particles are those emitted in the first decay and the low-energy alpha particles result from the decay of ^{8}Be. In general, the alpha spectra for channels 1 and 7 will not be very different; their variation as a function of the intermediate excited state is given in Figure 6. The shapes of these spectra are similar but the maximum energy of the spectra increases with increased intermediate excitation energy.

Similar results are given in Figure 7 for reaction channels NQ = 2 and NQ = 8. For the lower excited state, 2.43 MeV, the spectra again are not very different. The first alpha produced has a high energy and the spectrum is flat for both channels. When an intermediate state of 6.66 MeV is assumed, the results are quite different as now the first alpha produced will be low energy and the other two alpha particles will be of higher energy. In particular for NQ = 2, which consists of two two-body decays, the maximum alpha-particle energy will be much lower and the kerma will be correspondingly smaller.

The alpha-production spectra for a neutron energy of 14.1 MeV and for the four channels 3, 4, 5, and 6 are given on Figure 8. For channels 3, 4, and 6 which involve ^{5}He as an intermediate state, the spectra are not very different and the resulting kerma is approximately the same. For channel 5 there are more low-energy alpha particles in the spectrum which result from the decay of low-energy ^{8}Be and this results in a lower kerma.

5. THE EVENT-SIZE SPECTRA FOR DIFFERENT REACTION CHANNELS

The event size spectra for an inhomogeneous proportional counter were calculated at 14.1 MeV neutron energy for some of the different reaction channels to investigate whether a difference in event-size spectra could be used to distinguish various reaction mechanisms. Figure 9 gives the results for the reaction channels labeled 1 and 7. They differ only in that channel 1 involves two two-body decays while channel 7 involves a three-body decay. It would be difficult to distinguish between channels 1 and 7; in addition the shape of the spectra is very similar for all excited states of ^{12}C. The only difference for different excited states is that the area under the curve (the kerma) increases with increasing excitation energy. For these reasons, it would be difficult to distinguish experimentally between the two reaction channels or the different excited states. Figure 10 gives similar results for the reaction channels 2 and 8. Again it is seen that the shape of the event-size spectra are similar for all channels and that the only difference is the total area under the curve (or the contribution to the kerma). Obviously, it will be difficult to use the shape of the event-size spectra to distinguish different reaction channels, except that a shift of the peak toward lower event sizes will be an indication of increased numbers of higher-energy alpha particles.

6. CONCLUSION

Since recent experiments seem to indicate a kerma factor for carbon which is less than that which is obtained from using the data given in ENDF/B-V, a quick calculation was made to investigate how much the kerma factor for carbon could be lowered by using a different distribution of cross section among the various excited states of ^{12}C. In place of the distribution given by ENDF/B-V, a distribution was generated assuming that each excited state was equally probable except the probability for each state was zero below threshold and then increased linearly to full probability (equal with other states) over an interval of X MeV. A reasonable choice for the parameter X is

2 MeV. Figure 11 shows the results of such a calculation. The curve marked X = 2 MeV, shows the decrease in the kerma of the reaction $^{12}C(n,n')3\alpha$ for the more reasonable value for the parameter, X. The curve marked X = 100 MeV is an unrealistic extreme. Table IV gives the percent decrease in kerma for the $(n,n')3\alpha$ reaction and for the total kerma in carbon at a sample of the neutron energies used in the calculation. Again, the values given for X = 2 MeV are the most reasonable estimates.

At 14.1 MeV neutron energy and using the most reasonable estimate for X, this calculation produces only a 4% reduction in the total kerma; at 19 MeV it produces an 8% reduction. Since the reaction channel going through excited states of ^{12}C gives the lowest contributions to the $(n,n')3\alpha$ kerma, larger reductions in the carbon kerma could only be produced by a distribution of cross sections substantially different from those of ENDF/B-V. Consistency would then require a completely new evaluation of the carbon cross sections, since a study of uncertainties in all the cross sections and the correlations of these uncertainties would be needed. Furthermore, if the energy dependence of the contributing cross sections is also to be used, then optical model calculations must also be performed.

REFERENCES

1. ENDF/B Summary Documentation, BNL-NCS-17541 (ENDF-201), 3rd ed. (ENDF/B-V), R. Kinsey, Ed., National Nuclear Data Center, Brookhaven National Laboratory (1979).
2. ICRU, Neutron Dosimetry for Biology and Medicine, Report 26, Appendix A, pp. 74-90, International Commission on Radiation Units and Measurements, Washington, D.C., 1977.
3. R. S. Caswell, J. J. Coyne, and M. L. Randolph, Kerma Factors for Neutron Energies below 30 MeV, Rad. Res. 83, 217-254 (1980).

Table 1. The carbon cross sections for the various reaction channels shown in this table are given in terms of the percent of the total carbon cross section for neutron energies betweem E_n = 10.1 and 19.1 MeV. The total cross section, σ_T, is known to 2 percent and the elastic cross section, σ_e, is known to 3–5 percent. All of the other cross sections must add up to the difference $(\sigma_T - \sigma_e)$ to within some error that places limits on the upper-bound uncertainty that can be assumed for the (n,n') 3α reaction channel.

E_n (MeV)	Elastic	Inelastic	(n,p)+ (n,d)	(n,α)	(n,n')3α
19.1	63.9	5.7	5.8	2.9	21.7
18.1	60.1	6.9	5.7	3.1	24.1
17.1	59.3	7.6	4.0	3.7	25.4
16.1	58.5	8.8	2.1	4.5	26.0
15.1	61.7	11.3	0.1	5.6	21.3
14.1	61.1	14.3	-	6.2	18.4
13.1	64.3	15.3	-	6.7	13.8
12.1	63.6	16.1	-	7.2	13.1
11.1	59.5	24.8	-	5.7	9.9
10.1	53.6	28.4	-	15.0	3.0

Table 2 shows the percent of the total kerma for each of the reaction channels given in the first table; the data come from the ENDF/B-V carbon cross sections. Note that the (n,n')3α reaction channel is a large contributor to the kerma between 11 and 19 MeV; the (n,α) channel is also an important contributor and actually gives a larger contribution — per unit cross section — than any other reaction in this energy range.

E_n (MeV)	Elastic	Inelastic	(n,p)+ (n,d)	(n,α)	(n,n')3α
19.1	16.3	2.5	7.8	13.1	60.3
18.1	15.7	3.0	6.4	13.0	61.9
17.1	16.4	3.6	4.1	15.0	60.9
16.1	16.9	4.4	1.8	17.5	59.3
15.1	21.0	6.6	0.0	22.9	49.8
14.1	23.5	10.7	-	24.9	40.8
13.1	29.2	11.5	-	28.4	30.8
12.1	33.8	10.9	-	30.1	25.3
11.1	32.5	21.0	-	26.1	20.4
10.1	27.6	17.6	-	51.8	3.0

Table 3 shows the eight different reaction channels which can contribute to the (n,n')3α reaction (the four-body breakup channel of the intermediate ^{13}C compound state is excluded). Each one of these reaction channels gives a definite dependence of kerma on the neutron energy per unit cross section as well as a definite initial alpha-particle spectrum. Figures 1 through 3 show this kerma dependence while Figure 4 through 7 show the spectrum dependence. The notation for the reaction channel, NQ, is only a convenient numbering system for the various reaction channels.

Reaction Channel NQ	$n + {}^{12}C \rightarrow n + \alpha + \alpha + \alpha$	Q (MeV)
1	$n + {}^{12}C \rightarrow n' + {}^{12}C^*$	0.0
	$\alpha + {}^{8}Be$	- 7.3689
	$\alpha + \alpha$	+ 0.0947
2	$n + {}^{12}C \rightarrow \alpha + {}^{9}Be^*$	- 5.7038
	$n + {}^{8}Be$	- 1.6651
	$\alpha + \alpha$	+ 0.0947
3	$n + {}^{12}C \rightarrow \alpha + {}^{9}Be^*$	- 5.7038
	$\alpha + {}^{5}He$	- 2.5283
	$n + \alpha$	2.9578
4	$n + {}^{12}C \rightarrow {}^{5}He + {}^{8}Be$	- 8.3268
	$\alpha + \alpha$	0.0947
	$n + \alpha$	0.9578
5	$n + {}^{12}C \rightarrow n + \alpha + {}^{8}Be$	- 7.3689
	$\alpha + \alpha$	0.0947
6	$n + {}^{12}C \rightarrow \alpha + \alpha + {}^{5}He$	- 8.2321
	$n + \alpha$	0.9578
7	$n + {}^{12}C \rightarrow n + {}^{12}C$	0.0
	$\alpha + \alpha + \alpha$	- 7.2742
8	$n + {}^{12}C \rightarrow \alpha + {}^{9}Be^*$	- 5.7038
	$n + \alpha + \alpha$	- 1.5704

Table 4 shows the percent decrease in kerma for the $(n,n')3\alpha$ reaction as well as for the total kerma. As discussed in the text, X is a variable in the model that assumes a distribution of cross sections different from that given by ENDF/B-V. E_n is the energy of the incoming neutron in the reaction.

E_n (MeV)	X = 2 MeV		X = 100 MeV	
	$(n,n')3\alpha$	Total	$(n,n')3\alpha$	Total
19.1	13.9	8.4	26.3	15.9
18.1	13.5	8.3	25.3	15.7
17.1	11.5	7.0	23.0	14.0
16.1	12.2	7.2	23.0	13.6
15.1	11.8	5.9	22.2	11.1
14.1	10.0	4.1	21.0	8.6
13.1	7.9	2.4	20.0	6.1
12.1	5.4	1.4	17.0	4.3
11.1	23.0	4.8	28.0	5.8
10.1	1.0	0.0	1.5	0.0

Fig. 1 In this figure, the variation of kerma per unit neutron fluence and per unit cross section is given as a function of the neutron energy. The results for the reaction channels NQ = 1 and 7 (see Table 3) are the lines labeled with the excited-state energy of the ^{12}C nucleus. For comparison, the results for the reaction $^{12}C(n,\alpha)^{9}Be$ (where the ^{9}Be is left in the ground state) are shown along with the relatively weak contribution due to the elastic scattering.

Fig. 2 Is the same as in Fig. 1 except that the reaction channels are NQ = 2 (solid lines) and NQ = 8 (dashed lines). These channels are similar in that they involve intermediate excited-state products of ^{9}Be but differ in that channel 2 involves two two-body decays while channel 8 involves a three-body decay. Note that the difference in kerma factor between channel 2 and 8 is greater for the 6.66 MeV excited state as compared to the 2.43 MeV excited state.

Fig. 3 This figures shows the same data as Fig. 2 except that the reaction channels are NQ = 3, 4, 5, and 6. Except for NQ = 5, these channels involve ^{5}He as an intermediate state. The reaction channel NQ = 5 has the lowest threshold of all the reactions and is the closest to four-body break-up since there is only a small positive Q of .0947 MeV for the decay of ^{8}Be. This is the only reaction which can take place near threshold and the variation of the kerma factor is less than for the other reactions except for channels 1 and 7.

Fig. 4 shows the alpha-particle distribution (normalized to unity) versus the alpha-particle energy for 14.1 MeV neutrons for the reaction channels NQ = 1 and 7 when an excited state of 9.638 MeV in ^{12}C is assumed. The spectra for these two channels are only slightly different in shape. The reaction channels differ only in that Channel 7 involves a three-body decay while channel 1 has a series of two-body decays.

Fig. 5 is the same as that in Figure 4 except that a higher excitation energy of 12.25 MeV was used in the calculations. Note the more pronounced difference in shape. For the reaction channel NQ = 1, where there is a series of two two-body decays, the high-energy alpha particles are those emitted in the first decay and the low-energy alpha particles are those emitted from the second decay.

Fig. 6 shows how the alpha-particle spectra for 14.1 MeV neutrons varies as a function of the intermediate excited state. The shape of the spectra are similar but the maximum energy increases with increasing intermediate excitation energy.

Fig. 7 is similar to the data plotted in Figure 4 and 5 except that the reaction channel shown here is for NQ = 2 and 8 and the excited state is 2.43 and 6.66 MeV. For the lower excited states the spectra are again not very different because the first alpha particle produced is of high energy and the spectrum is flat for both channels. This contrasts with the results obtained when an intermediate state of 6.66 MeV is assumed. The results are quite different as now the first alpha particle will be low energy and the other two alpha particles will be of higher energy.

Fig. 8 shows the distribution of alpha particles at a neutron energy of 14.1 MeV for the reaction channels NQ = 3, 4, 5, and 6. All channels, except 5, involve ^{5}He as an intermediate state and the spectra and kerma are not very different. For channel 5, there are more low-energy alpha particles in the spectrum resulting from the decay of a low-energy ^{8}Be and this results in a lower kerma.

Fig. 1

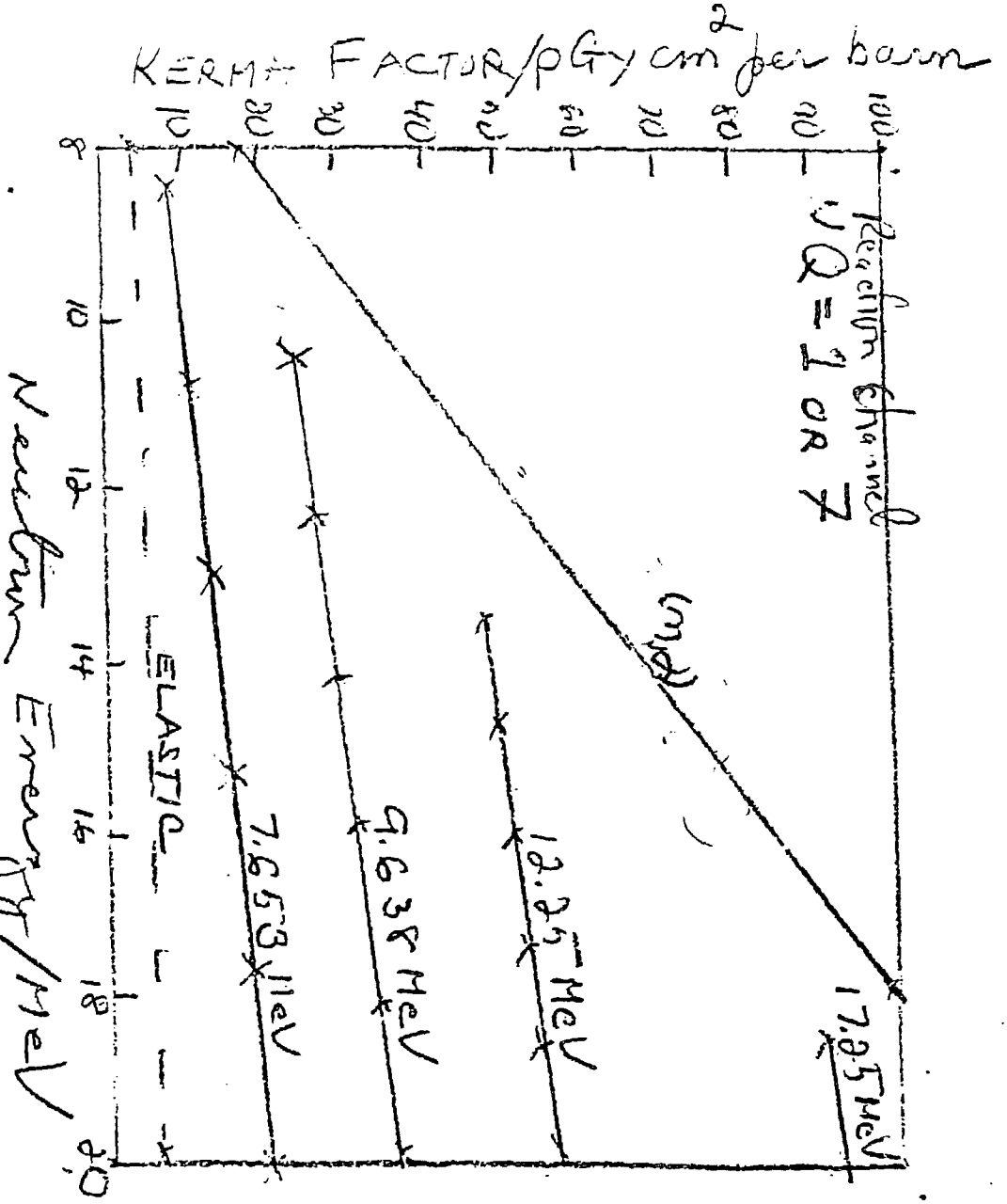
KERMA FACTOR/pGy cm² per barn
Reaction Channel
Q = 1 OR 7
17.95 MeV
12.25 MeV
9.638 MeV
7.653 MeV
ELASTIC
Neutron Energy/MeV
100
90
80
70
60
50
40
30
20
10
8
10
12
14
16
18
20

Figure 2

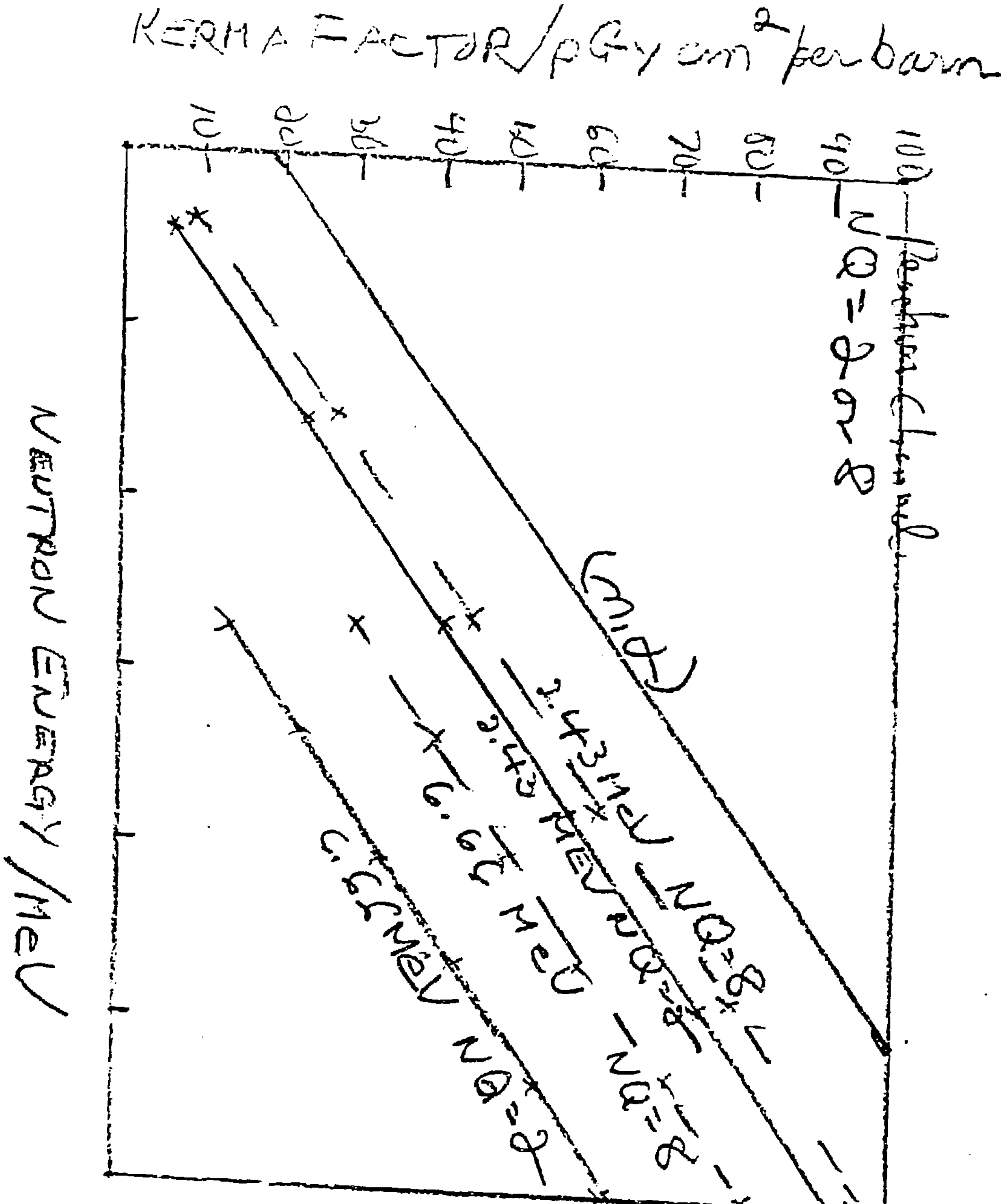

Figure 3

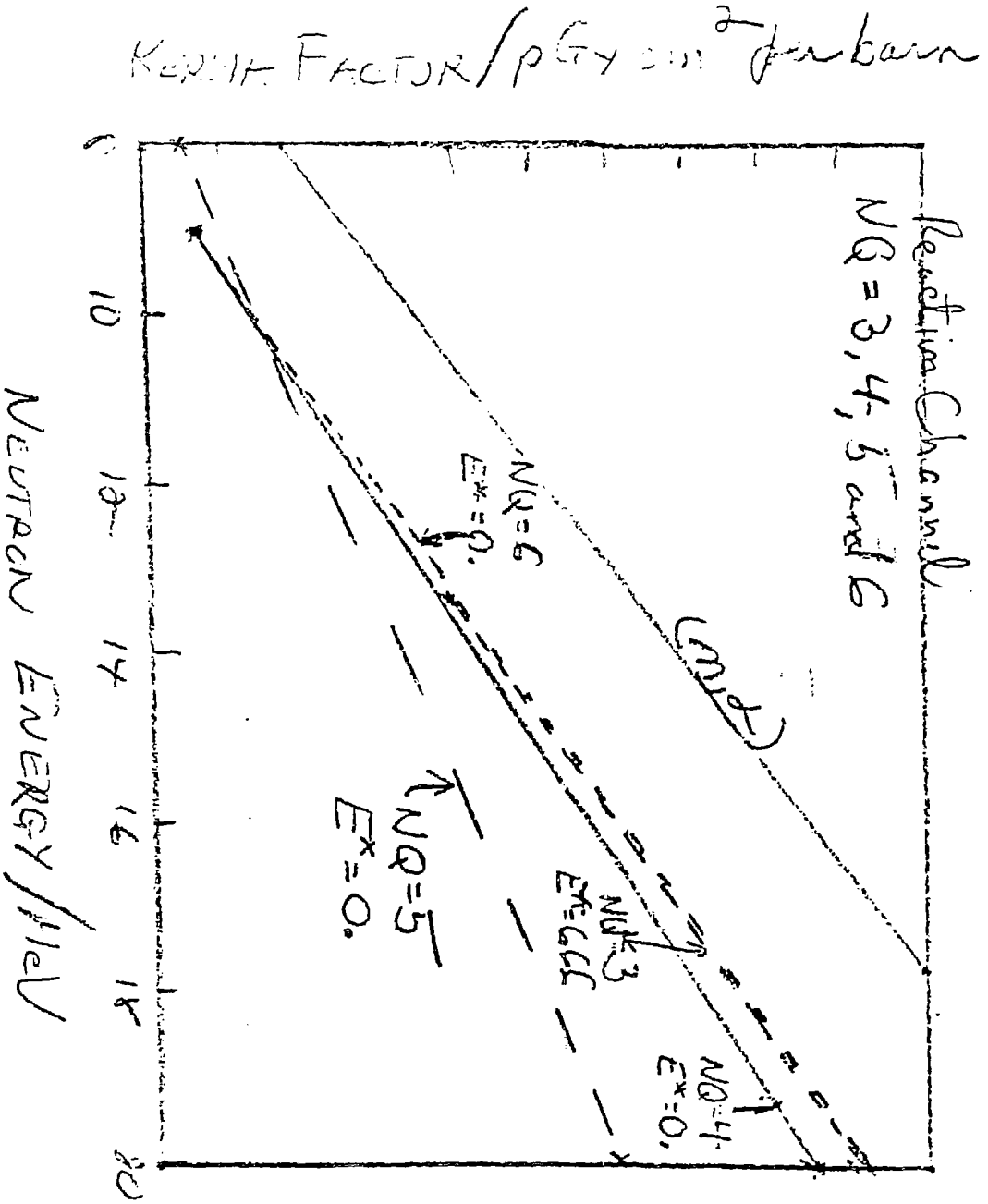
KERMA FACTOR/pGy cm² fm barn
Reaction Channel
NQ = 3, 4, 5 and 6
(mod)
NQ=6
E*=0.
NQ=3
E*=6.66
NQ=4
E*=0.
NQ=5
E*=0.
10
12
14
16
18
20
NEUTRON ENERGY/MeV

Fig 4

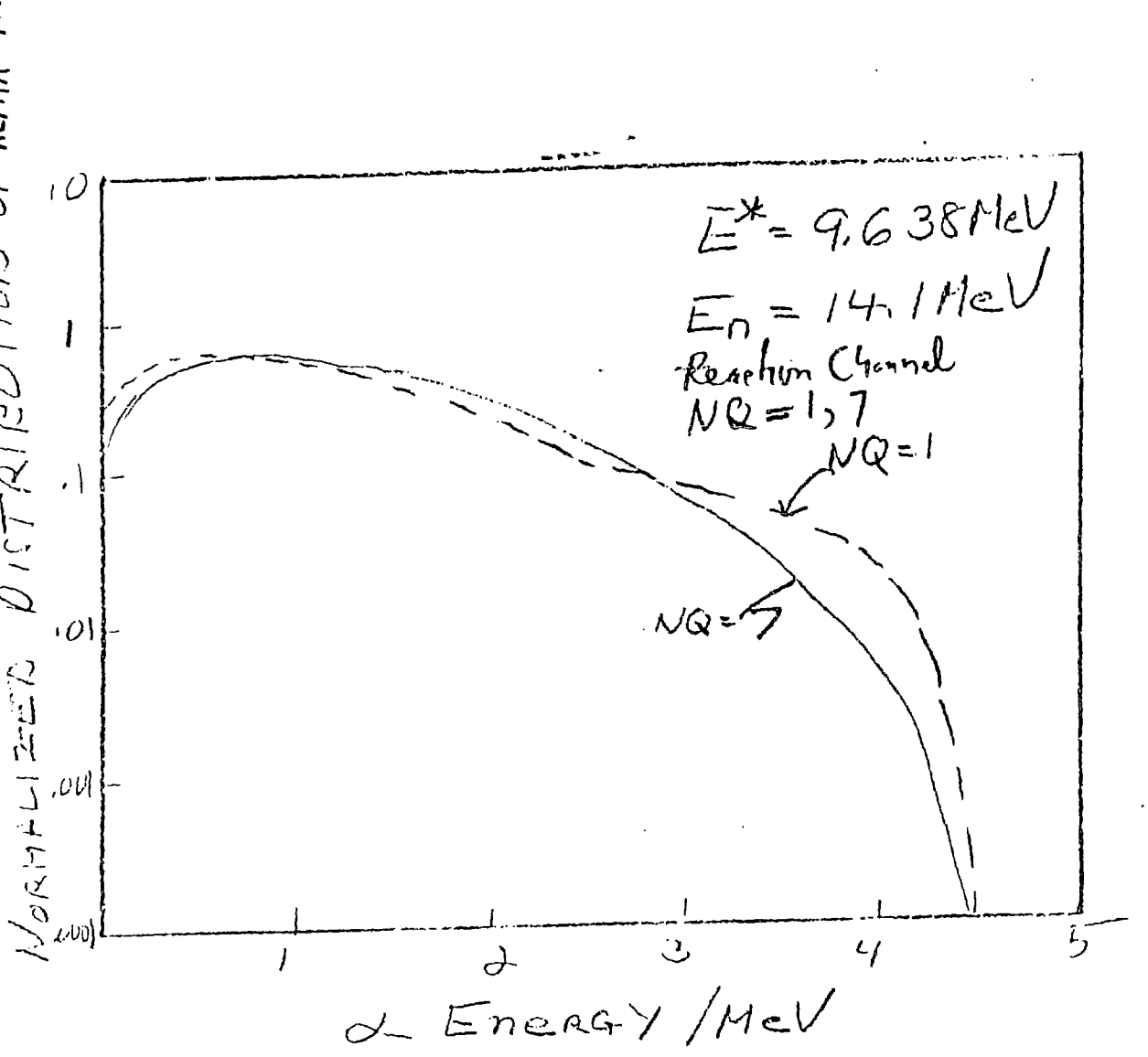
NORMALIZED DISTRIBUTION OF ALPHA P
10
1
.1
.01
.001
1
2
3
4
5
α ENERGY /MeV
E* = 9.638 MeV
En = 14.1 MeV
Reaction Channel
NQ = 1, 7
NQ = 1
NQ = 7

Fig 5

NORMALIZED DISTRIBUTION
10
1
0.1
0.01
1
2
3
4
5
6
7
α ENERGY / MeV
E* = 12.25 MeV
Eη = 14.1 MeV
Resolution Channel NQ=1,7
NQ=1
NQ=7

Fig 6

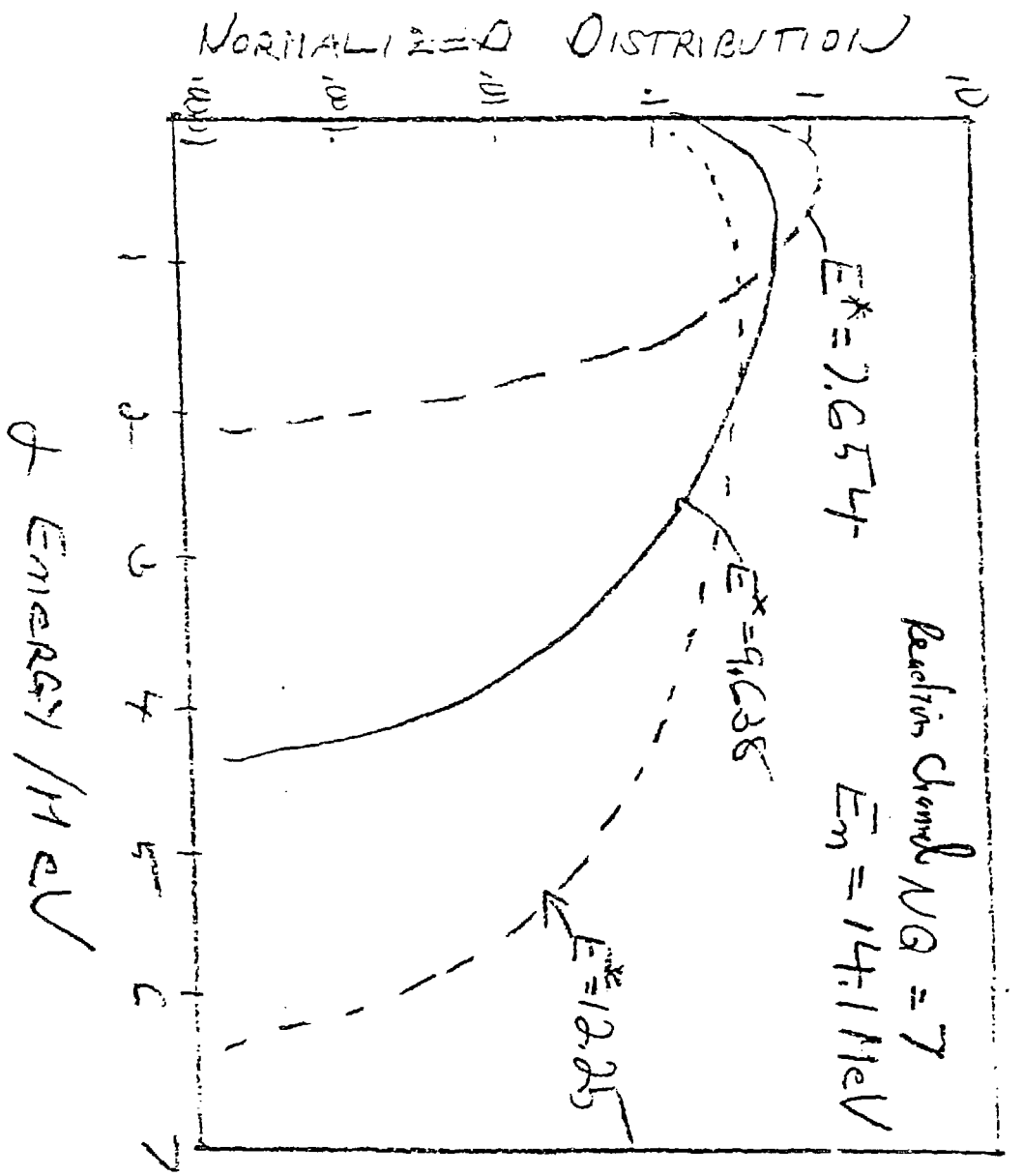
NORMALIZED DISTRIBUTION
Reaction Channel NQ = 7
E_n = 14.1 MeV
E^* = 7.654
E^* = 9.636
E^* = 12.25
Energy / MeV

Figure 7

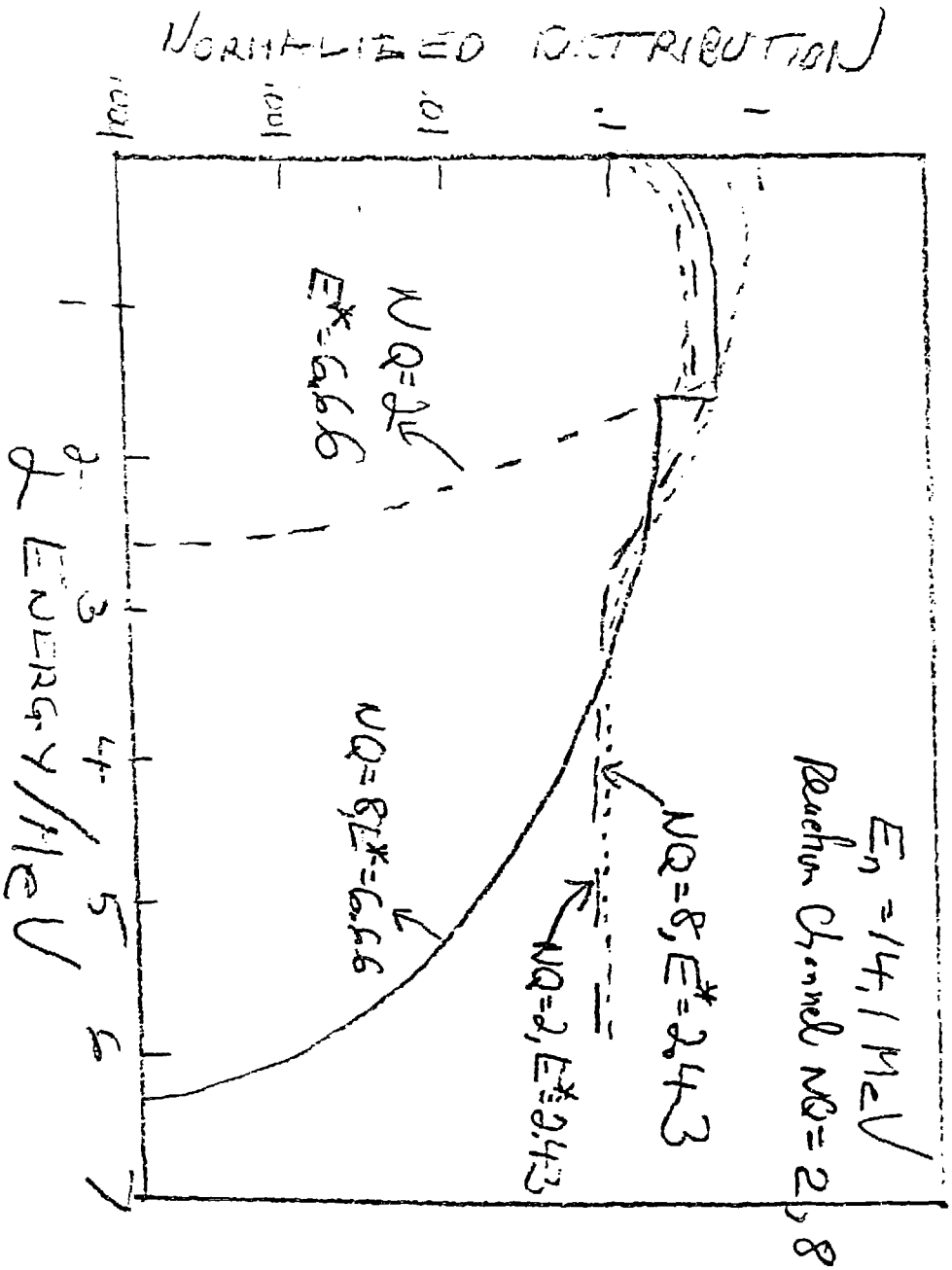
NORMALIZED DISTRIBUTION
E_n = 14.1 MeV
Reaction Channel NQ = 2, 8
NQ=8, E*=2.43
NQ=2, E*=0.43
NQ=8, E*=6.66
NQ=2, E*=6.66
ENERGY / MeV

Figure 8

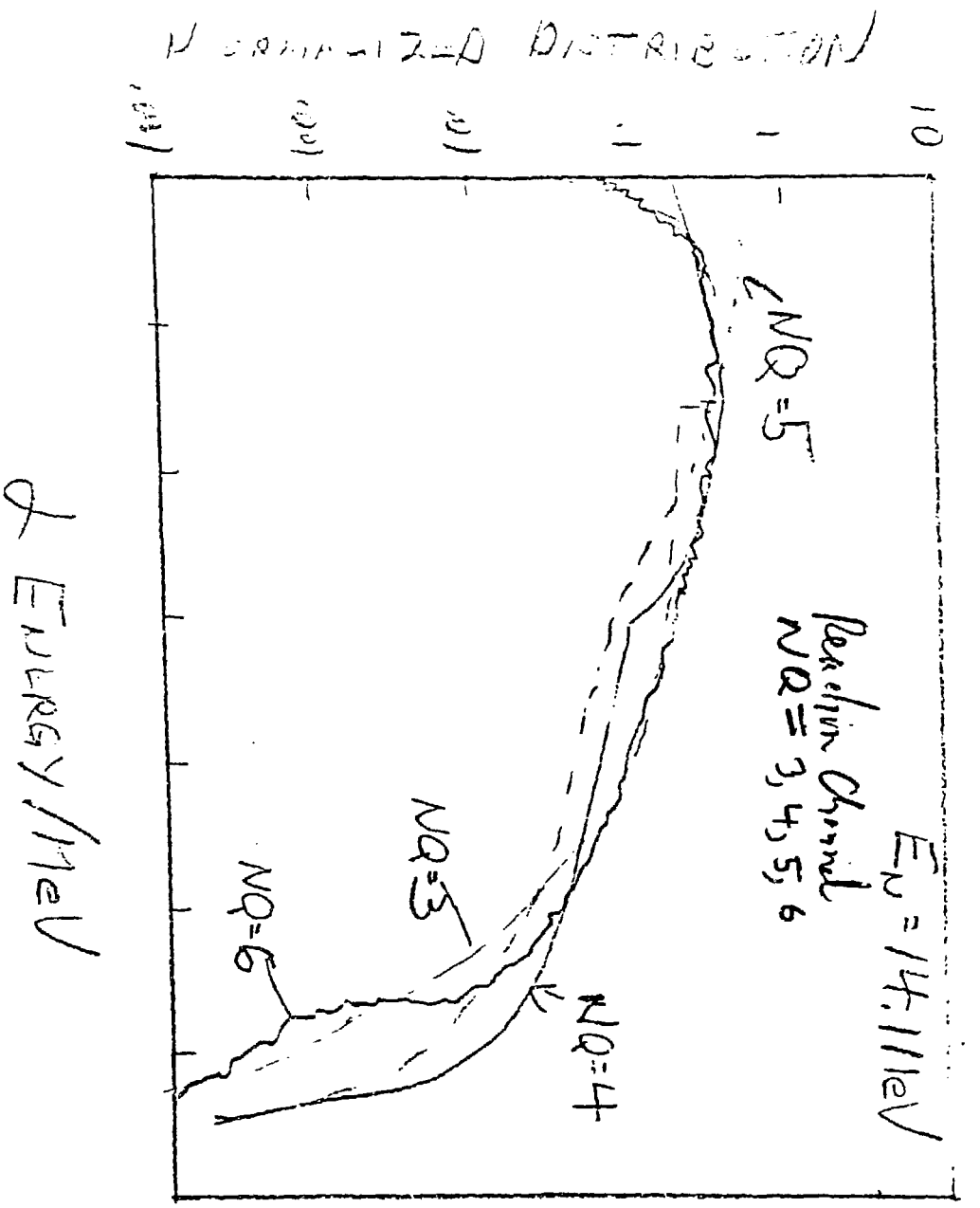
NORMALIZED DISTRIBUTION
10
1
0.1
0.01
E_N = 14.111eV
Resolution Channel
NQ = 3, 4, 5, 6
NQ=5
NQ=3
NQ=6
NQ=4
ϵ ENERGY / MeV

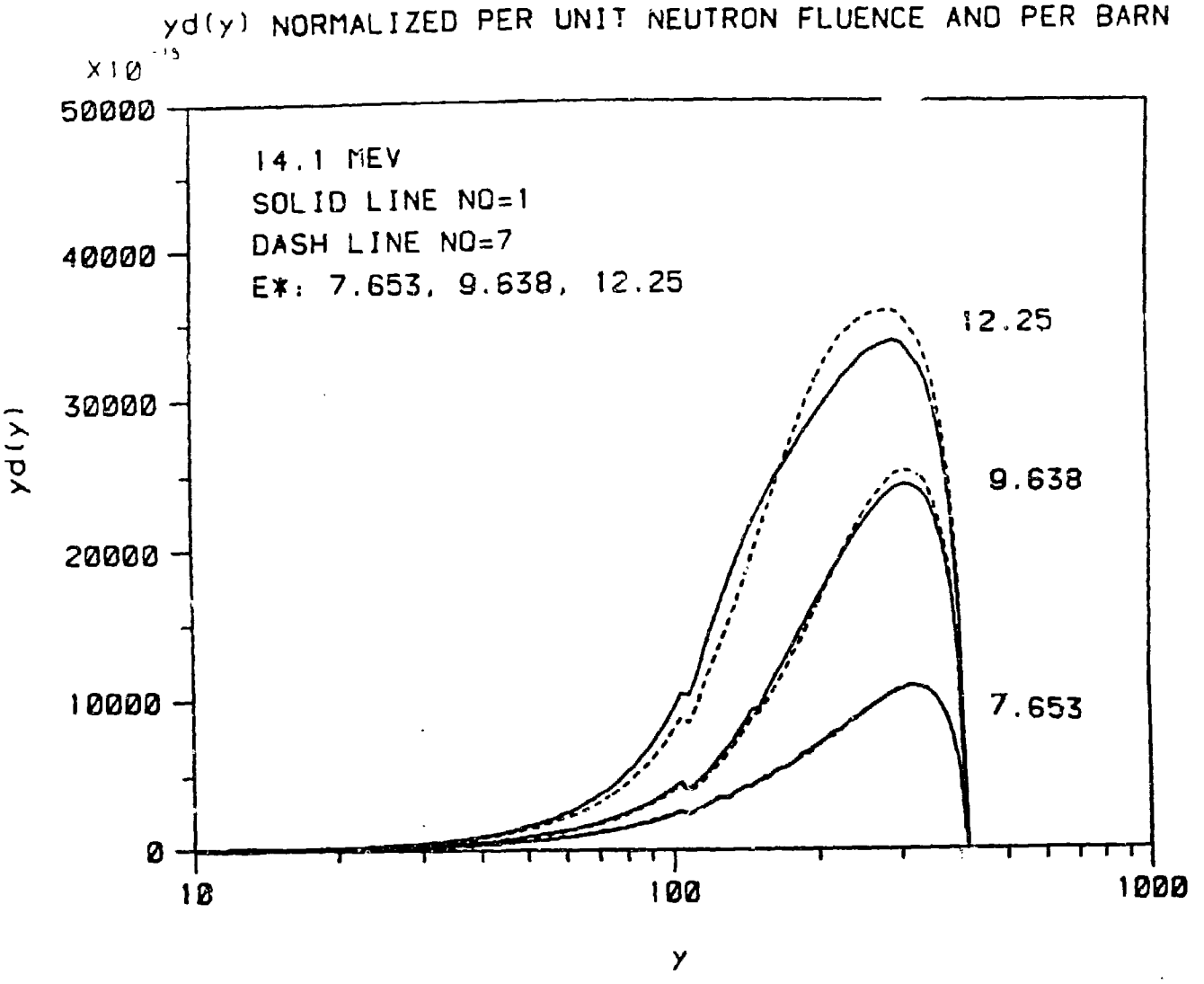

Fig. 9 shows the calculated event-size spectra for an inhomogeneous proportional counter at 14.1 MeV neutron energy. The lineal energy, y, times the dose probability density, d(y), is plotted as a function of the log of the linear energy. yd(y) is normalized per unit neutron fluence and per barn. The results are given for reaction channels NQ = 1 and 7 for the ^{12}C nucleus in three different excited states. Channel 1 involves two two-body decays while channel 7 involves a three-body decay. Since the shape of the curves for all excited states is similar, it would be difficult to tell experimentally if the two-body or the three-body decay mechanism was operating. The biggest difference for the various excited states is that the area under the curve, the kerma, is increasing with increasing excitation energy.

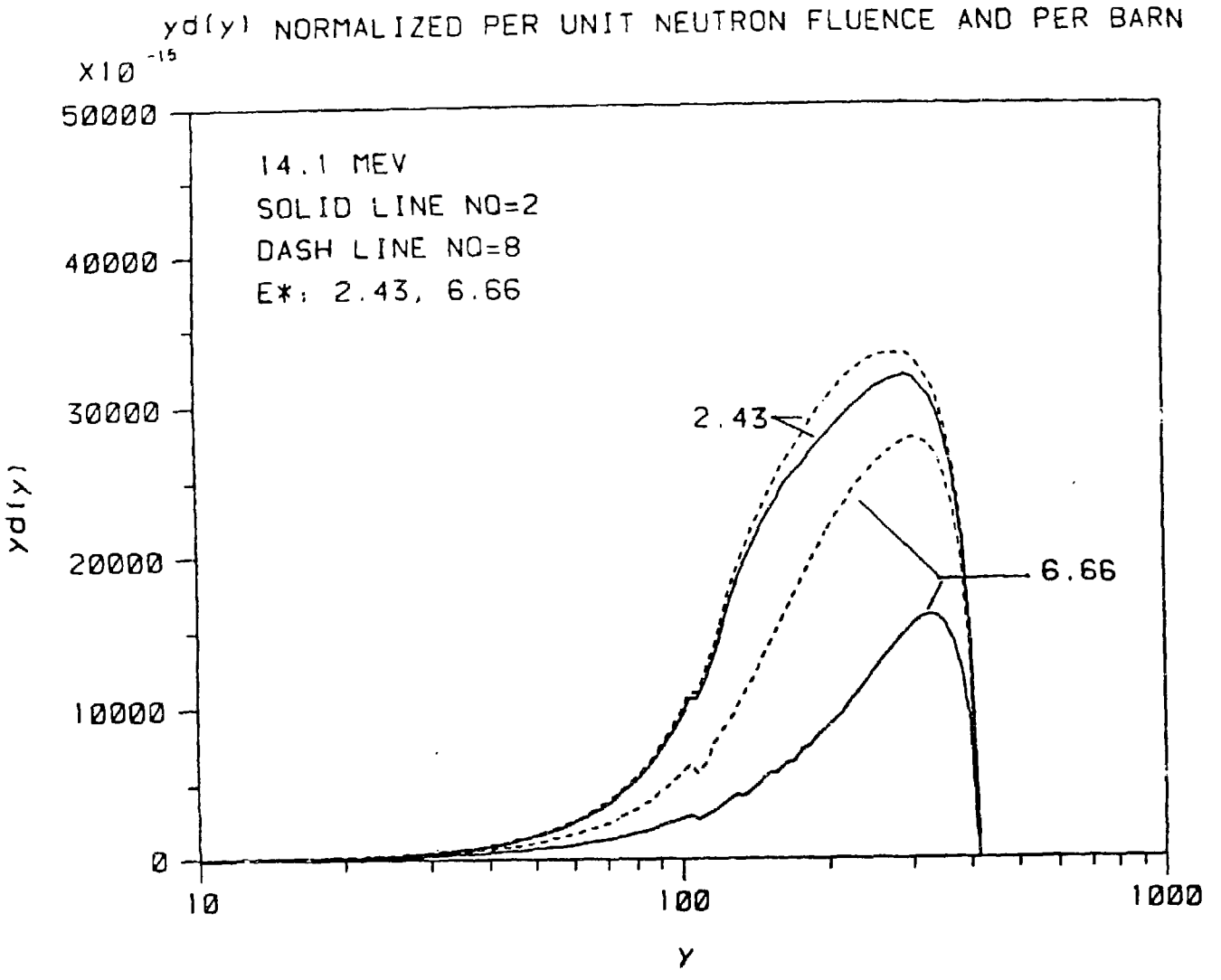

Fig. 10. The data in this figure is the same as that in Figure 9 except that the reaction channels are NQ = 2 and 8 and the excited states of the ^{9}Be nucleus are 2.43 and 6.66 MeV. As with the data in Figure 9, it is seen that the shape of the event size spectra are similar for all channels and thus it is difficult to use the shape variations to distinguish between the different reaction mechanisms.

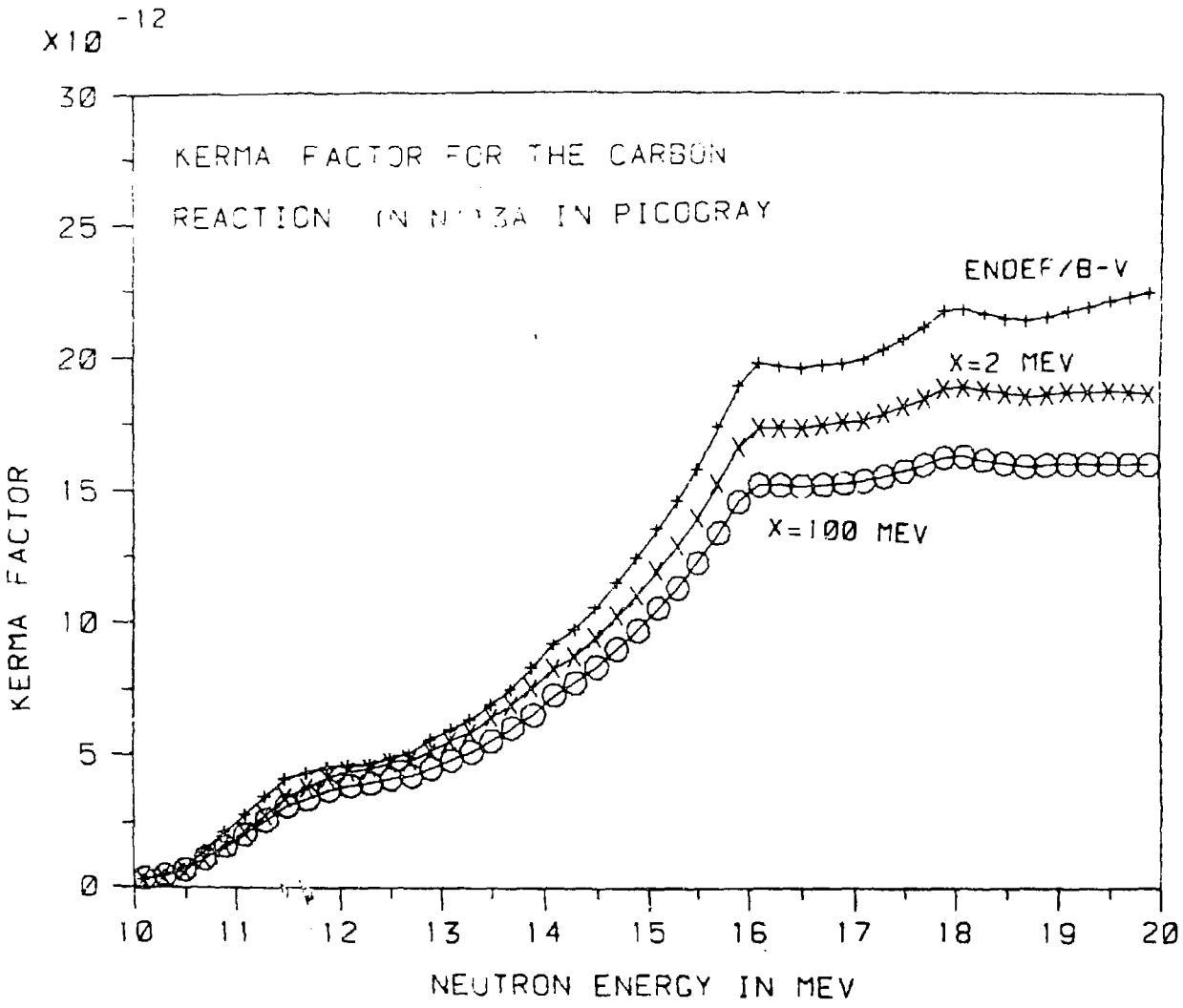

Fig. 11. The curve marked ENDF/B-V shows the kerma factor variation for the $^{12}C(n,n')3\alpha$ reaction as a function of neutron energy. The curve was calculated using the data given in ENDF/B-V. Since recent experiments indicate a kerma factor for carbon less than that which is obtained using the ENDF/B-V data, a calculation was made to see if the kerma factor could be reduced by using a different distribution of cross sections for the reactions in ^{12}C. A model was used that assumed each excited state was equally probable except that the probability for each state was zero below threshold and increased linearly to full probability over an interval of X MeV. The middle curve shows the decrease in the kerma factor for the $^{12}C(n,n')3\alpha$ reaction when X = 2 MeV is used in the model. The lower curve shows the results for X = 100 MeV. Although these changes are in the right direction to reduce the discrepancy with the measured data, the magnitude of the change is not enough to explain the difference.